An Accurate Power-sharing Control Method based on Circulating-current Power Model for Voltage-source-inverter Parallel System

Mingzhi Gao, Canhui Zhang, Maohang Qiu, Weiheng Li, Min Chen, Zhaoming Qian
Department of Applied Electronics, College of Electrical Engineering
Zhejiang University
Hangzhou, China
xiaosan433@zju.edu.cn

***Abstract*—This paper analyzes the voltage-source-inverter parallel system as a multi-input & multi-output system, and proposes the circulating-current mathematical model, the steady-state model and small-signal model of parallel system. Then the phasor models of the circulating-current and the circulating-current power are proposed. Subsequently, the mathematical model of traditional droop control is built and analyzed based on the circulating-current power model. According to the analysis of droop control, this paper proposes an accurate parallel control strategy ($\omega-P_{cir}$ and $V-Q_{cir}$ control), which can eliminate the circulating-current power and the bias of output voltage frequency and amplitude. Finally, simulation and experiment result are presented, which validates the performance of the proposed method.**

Keywords—Voltage-source Inverter; Parallel system; Droop control; Circulating-current

I. INTRODUCTION

Droop control is a classical control strategy of voltage-source-inverter parallel system (VSIPS), which has excellent robustness and expansibility since communication can be avoided [1,2]. However, it has a trade-off between steady-state voltage error and load sharing accuracy [3].

The theoretical model of traditional droop control is analyzed in many references [4-6]. In this model, the voltage-source inverters (VSI) and the AC bus are equivalent to ideal voltage source. Every VSI is conceived and treated as a separate entity, and only the relationship of VSI and AC bus is analyzed. Moreover, droop control didn't elaborate the mathematical model of circulating current, and the mechanism of circulating-current eliminating is not clear.

In fact, VSIPS should be a multi-input & multi-output system, which needs to be analyzed as an organic whole. System's inputs are VSI voltages, and system's outputs are inverters' output currents. Users' load is an uncontrollable variable, and AC bus voltage is a state variable of VSIPS.

Based on this conclusion, the mathematical model of circulating current, the steady-state model and small-signal model of VSIPS are proposed by analyzing the equivalent circuit diagram of VSIPS in Section II. Subsequently, the phasor models of circulating current and circulating-current power are proposed in Section III.

According to the proposed circulating-current power model, the mathematical model of droop control is built and analyzed in Section IV. Based on this model, the steady-state voltage error and the mechanism of the circulating-current eliminating in droop control are both analyzed, which elaborate the trade-off between steady-state voltage error and load sharing accuracy, and prove that $V-Q$ droop control can't realize accurate reactive-power sharing.

According to the analysis in Section IV, an accurate power-sharing control method ($\omega-P_{cir}$ and $V-Q_{cir}$ control) based on the circulating-current power model is proposed in Section V. The model of the proposed method is built and analyzed subsequently, which proves that this method can avoid the steady-state voltage error and realize accurate power sharing. Meanwhile, the optimum droop coefficient of this method is also designed based on this model.

Finally, simulation and experiment results based on parallel-inverter system are presented in Section VI and VII, which validates the performance of the proposed method.

II. PROPOSED MATHEMATICAL MODEL OF VSIPS

A. Proposed mathematical model of the circulating-current

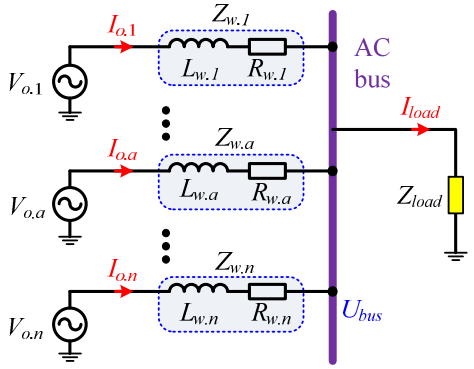

Fig. 1. Equivalent circuit diagram of VSIPS

This work was supported by National Natural Science Foundation of China (Project 51107116).

Fig. 1 expresses the equivalent circuit diagram of VSIPS, which consists of n inverters. $V_{o.a}$ and $I_{o.a}$ is the output voltage and current of the inverter which is numbered a. $Z_{w.a}$ is the wire impedance between every inverter and AC bus. I_{load} is the current of the common load Z_{load}. AC bus voltage U_{bus} can be expressed as (1), which shows that U_{bus} is a state variable of VSIPS and controlled by $V_{o.a}$.

$$U_{bus}(s)=\frac{\frac{V_{o.1}(s)}{Z_{w.1}}+\frac{V_{o.2}(s)}{Z_{w.2}}+\ldots+\frac{V_{o.n}(s)}{Z_{w.n}}}{\frac{1}{Z_{load}}+\frac{1}{Z_{w.1}}+\frac{1}{Z_{w.2}}+\ldots+\frac{1}{Z_{w.n}}} \tag{1}$$

In VSIPS, the circulating current of every inverter can be defined as the difference of $I_{o.a}$ and theoretical output current $I_{t.a}$, as shown in (2). And the expression of $I_{o.a}$ and $I_{t.a}$ can be shown in (3), k_a is the proportion of $I_{t.a}$ in I_{load}, which is also the weight coefficient of every inverter in load-power sharing. Therefore, k_a should satisfy the relationship of (4)

$$I_{cir}(s)=I_o(s)-I_t(s) \tag{2}$$

$$\begin{cases} I_{o.a}(s)=\dfrac{V_{o.a}(s)-U_{bus}(s)}{Z_{w.a}} \\ I_{t.a}(s)=k_a\cdot I_{load}(s) \end{cases} \quad a=1\ldots n \tag{3}$$

$$\sum_{j=1}^{n}k_j=1 \tag{4}$$

By substituting (1), (3) and (4) into (2), $I_{cir.a}$ can be expressed as (5). According to this equation, $I_{cir.a}$ is controlled by the inverters' output voltages, and it is also affected by the load and wire impedance.

$$I_{cir.a}(s)=\frac{V_{o.a}(s)}{Z_{w.a}}-\left(\frac{\frac{1}{Z_{w.a}}+\frac{k_a}{Z_{load}}}{\sum_{j=1}^{n}\frac{1}{Z_{w.j}}+\frac{1}{Z_{load}}}\right)\cdot\sum_{j=1}^{n}\frac{V_{o.j}(s)}{Z_{w.j}} \tag{5}$$

If $Z_{w.a}$ satisfies the relation of (6), then (5) can be simplified into (7). In this equation, V_m equals to the weighted average of all inverter output voltage in VSIPS, as shown in (8).

$$k_a\cdot Z_{w.a}=k_j\cdot Z_{w.j}=1\cdot Z_e \quad a,j=1\ldots n \tag{6}$$

$$I_{cir.a}(s)=\frac{V_{o.a}(s)-V_m(s)}{Z_{w.a}} \tag{7}$$

$$V_m(s)=\sum_{j=1}^{n}\left[k_j\cdot V_{o.j}(s)\right] \tag{8}$$

Equation (7) is the proposed mathematical model of circulating current. According to this model, $I_{cir.a}$ is caused by the difference of $V_{o.a}$ and V_m, when $Z_{w.a}$ satisfies the relation of (6). Meanwhile, the influence of Z_{load} on $I_{cir.a}$ is eliminated.

B. *Proposed steady-state model of VSIPS*

In the steady state, the circulating-current equals to zero approximately due to the effect of parallel control strategy. So $V_{o.a}$ equals to V_m according to (7). Therefore, the steady-state model of VSIPS can be obtained as shown in Fig. 2. The steady-state model of every inverter can be shown in Fig. 3, and Z_{load}/k_a is the shared load of every inverter.

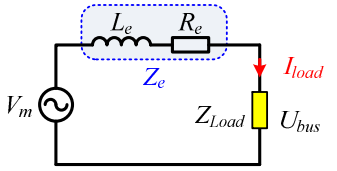

Fig. 2. Steady-state model of VSIPS

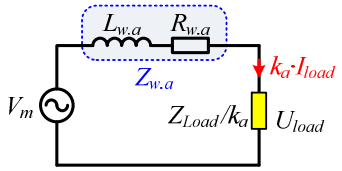

Fig. 3. Steady-state model of one inverter

C. *Proposed small-signal model of VSIPS*

Small-signal model can be obtained based on the steady-state model. $V_{o.a}$ can be expressed as (9), in which $\Delta V_{o.a}$ is the disturbing signal of $V_{o.a}$. $I_{cir.a}$ is recognized as the small-signal of $I_{o.a}$, as shown in (10). According to (10), $I_{cir.a}$ is caused by small-signal disturbance of $\Delta V_{o.a}$. Therefore, the small-signal model of VSIPS can be shown in Fig. 4, and the circulating-current small-signal model can be shown in Fig. 5.

$$V_{o.a}(s)=V_m(s)+\Delta V_{o.a}(s) \tag{9}$$

$$I_{cir.a}(s)=\frac{\Delta V_{o.a}(s)}{Z_{w.a}}=\frac{\Delta V_{o.a}(s)}{Z_e/k_a} \tag{10}$$

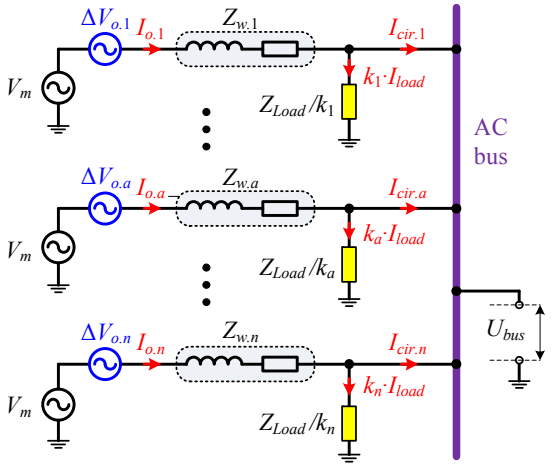

Fig. 4. Small-signal model of VSIPS

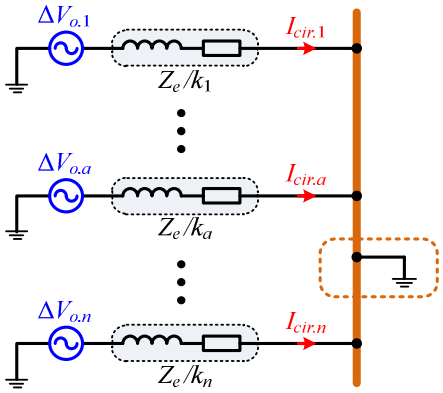

Fig. 5. Small-signal model of circulating-current

III. Proposed Phasor Model of Circulating-Current and Circulating-Current Power

A. Phasor model of circuating-current

In the phasor model, the relationship of $V_{o.a}$ and V_m as shown in (8) can be expressed as (11). V_A is the RMS voltage of V_m, and the phase of V_m is defined as 0. $V_{rms.a}$ is the RMS voltage of $V_{o.a}$, and θ_a is phase difference of $V_{o.a}$ and V_m. In the steady state, θ_a and ($V_{rms.a}$−V_A) equal to 0 approximately, so (11) can be simplified into (12).

$$\begin{aligned} V_A\angle 0 &= \sum_{i=1}^{n}\left(k_i\cdot V_{rms.i}\angle\theta_i\right) \\ &= \sum_{i=1}^{n}\left(k_i\cdot V_{rms.i}\cos\theta_i\right)+j\sum_{i=1}^{n}\left(k_i\cdot V_{rms.i}\sin\theta_i\right) \end{aligned} \tag{11}$$

$$\begin{cases} \sum_{i=1}^{n}\left(k_i\cdot V_{rms.i}\right)=V_A \\ \sum_{i=1}^{n}\left(k_i\cdot\theta_i\right)=0 \end{cases} \tag{12}$$

Moreover, the wire impedance is defined as $Z_{w.a}\angle\phi_{w.a}$, which satisfies the relation of (13). Therefore, the phasor model of $I_{cir.a}$ can be obtained as shown in (14) and (15) by subsisting the phasor expression of $V_{o.a}$, V_m and $Z_{w.a}$ into (7).

$$k_a\cdot Z_{w.a}\angle\phi_{w.a}=Z_e\angle\phi_e=R_e+j\omega L_e \quad a=1...n \tag{13}$$

$$\vec{I}_{cir.a}=I_{cir.a.p}+j\cdot I_{cir.a.q} \tag{14}$$

$$\begin{cases} I_{cir.a.p}=\dfrac{\left(V_{rms.a}-V_A\right)\cos\phi_e+\theta_a\cdot V_{rms.a}\sin\phi_e}{Z_{w.a}} \\ I_{cir.a.q}=\dfrac{\theta_a\cdot V_{rms.a}\cos\phi_e-\left(V_{rms.a}-V_A\right)\sin\phi_e}{Z_{w.a}} \end{cases} \tag{15}$$

According to this model, $I_{cir.a.p}$ and $I_{cir.a.q}$ is controlled by voltage difference "$V_{rms.a}$−V_A" and phase difference θ_a. This coupling relationship is determined by the wire impedance phase ϕ_e. When ϕ_e is 0° (Resistive impedance) or 90° (Inductive impedance), (15) can be simplified as shown in (16).

$$\begin{cases} \vec{I}_{cir.a}=\dfrac{V_{rms.a}-V_A}{Z_{w.a}}+j\cdot\dfrac{\theta_a\cdot V_{rms.a}}{Z_{w.a}} & \phi_e=0^\circ \\ \vec{I}_{cir.a}=\dfrac{\theta_a\cdot V_{rms.a}}{Z_{w.a}}-j\cdot\dfrac{V_{rms.a}-V_A}{Z_{w.a}} & \phi_e=90^\circ \end{cases} \tag{16}$$

B. Phasor model of circluating current power

According to the proposed mathematical model in Section II, the phasor model of inverter's output power $S_{o.a}$ can be expressed as (17). In this equation, S_{to} is the total output power of VSIPS, which is expressed as (18). Therefore, the active power $P_{o.a}$ and reactive power $Q_{o.a}$ of any inverter can be expressed as (19). In this equation, P_{to} and Q_{to} are the total active and reactive power of VSIPS. According to (17) and (19), the circulating-current power $S_{cir.a}$ can be recognized as the small-signal of output power $S_{o.a}$.

$$\begin{aligned} \vec{S}_{o.a} &= \vec{V}_{o.a}\cdot\vec{I}_{o.a}^{*}=\left(\vec{V}_m+\Delta\vec{V}_{o.a}\right)\cdot\left(k_a\cdot\vec{I}_{load}+\vec{I}_{cir.a}\right)^{*} \\ &= k_a\cdot\vec{S}_{to}+\vec{S}_{cir.a} \end{aligned} \tag{17}$$

$$\vec{S}_{to}=\vec{V}_m\cdot\vec{I}_{load}^{*}=\sum_{i=1}^{n}\vec{S}_{o.i} \tag{18}$$

$$\begin{cases} P_{o.a}=k_a\cdot P_{to}+P_{cir.a}=k_a\cdot\sum_{i=1}^{n}P_{o.i}+P_{cir.a} \\ Q_{o.a}=k_a\cdot Q_{to}+Q_{cir.a}=k_a\cdot\sum_{i=1}^{n}Q_{o.i}+Q_{cir.a} \end{cases} \tag{19}$$

According to (17), the expression of $S_{cir.a}$ can be obtained as shown in (20) and (21) after simplification.

$$\vec{S}_{cir.a}=P_{cir.a}+jQ_{cir.a} \tag{20}$$

$$\begin{cases} P_{cir.a}=\left(V_{rms.a}-V_A\right)\cdot k_a\cdot V_A\cdot\left(\dfrac{1}{\vec{Z}_e^{*}+\vec{Z}_{load}^{*}}+\dfrac{1}{\vec{Z}_e^{*}}\right) \\ Q_{cir.a}=\theta_a\cdot k_a\cdot V_A^2\cdot\left(\dfrac{1}{\vec{Z}_e^{*}+\vec{Z}_{load}^{*}}-\dfrac{1}{\vec{Z}_e^{*}}\right) \end{cases} \tag{21}$$

According to (21), $S_{cir.a}$ is affected by Z_{load}. But the influence of Z_{load} can be eliminated when Z_e is far less than Z_{load}. Therefore, (21) can be simplified into (22).

$$\begin{cases} P_{cir.a}=\dfrac{k_aV_A}{\omega^2L_e^2+R_e^2}\left[R_e\left(V_{rms.a}-V_A\right)+\theta_aV_A\omega L_e\right] \\ Q_{cir.a}=\dfrac{k_aV_A}{\omega^2L_e^2+R_e^2}\left[\omega L_e\left(V_{rms.a}-V_A\right)-\theta_aV_AR_e\right] \end{cases} \tag{22}$$

Equation (22) is the proposed phasor model of circulating-current power in this paper. It elaborated that, $P_{cir.a}$ and $Q_{cir.a}$ is

controlled by the voltage difference "$V_{rms.a}-V_A$" and phase difference θ_a, when $Z_e << Z_{load}$. This coupling relationship is determined by the wire impedance phase ϕ_e. When ϕ_e equals to 0° or 90°, (22) can be simplified as (23).

$$\begin{cases} \vec{S}_{cir.a} = \dfrac{k_a V_A}{R_e}\cdot\left(V_{rms.a}-V_A\right) - j\dfrac{k_a V_A^2}{R_e}\cdot\theta_a & \phi_e = 0^\circ \\ \vec{S}_{cir.a} = \dfrac{k_a V_A^2}{\omega L_e}\cdot\theta_a - j\dfrac{k_a V_A}{\omega L_e}\cdot\left(V_{rms.a}-V_A\right) & \phi_e = 90^\circ \end{cases} \tag{23}$$

IV. Model of Traditional Droop Control

In traditional droop control, $\omega-P$ control and $V-Q$ control adjust the frequency and amplitude of voltage in every control cycle as shown in (24). ω^* and V^* are the rated angular frequency and RMS value of $V_{o.a}$, $m_{\omega.a}$ and $n_{v.a}$ are the droop coefficients of any inverter, which satisfy the relation of (25). $m_{\omega.e}$ and $n_{v.e}$ are defined as the equivalent droop coefficient.

$$\begin{cases} \omega_{a.k} = \omega^* - m_{\omega.a}\cdot P_{o.a.k-1} \\ V_{a.k} = V^* - n_{v.a}\cdot Q_{o.a.k-1} \end{cases} \tag{24}$$

$$\begin{cases} m_{\omega.a}\cdot k_a = m_{\omega.j}\cdot k_j = m_{\omega.e} \\ n_{v.a}\cdot k_a = n_{v.j}\cdot k_j = n_{v.e} \end{cases} \quad a,j = 1...n \tag{25}$$

In (6), k is the number of control cycle. $P_{o.a.k\text{-}1}$ and $Q_{o.a.k\text{-}1}$ are active and reactive output power of any inverter in the $(k-1)^{th}$ cycle. $\omega_{a.k}$ and $V_{a.k}$ are the angular frequency and RMS value adjusted by droop control in the k^{th} cycle. Moreover, droop control begins to work from the 1st cycle, so $\omega_{a.0}$ and $V_{a.0}$ equal to ω^* and V^*.

Moreover, $\omega-P$ control can be changed to (26) in phasor model. $T_{c.\omega}$ is the time of $\omega-P$ control cycle. $\theta_{a.k}$ is the adjusted phase by droop control in the k^{th} cycle, and $\theta_{a.0}$ equals to the initial phase of any inverter which is θ_a. Meanwhile, there exists voltage deviation among inverters, so V^* in (24) should be replaced with $V_{rms.a}$ in phasor model, as shown in (27).

$$\theta_{a.k} = \theta_{a.k-1} - m_{\omega.a}\cdot T_{c.\omega}\cdot P_{o.a.k-1} \tag{26}$$

$$V_{a.k} = V_{rms.a} - n_{v.a}\cdot Q_{o.a.k-1} \tag{27}$$

According to the circulating-current power model, (28) can be obtained by substituting (19) into (26) and (27). In (28), $P_{cir.a.k\text{-}1}$ and $Q_{cir.a.k\text{-}1}$ are the circulating current power in the $(k-1)^{th}$ cycle. P_{to} and Q_{to} are recognized as constants in the steady state.

$$\begin{cases} \theta_{a.k} = \theta_{a.k-1} - m_{\omega.e}\cdot T_{c.\omega}\cdot P_{to} - m_{\omega.a}T_{c.\omega}\cdot P_{cir.a.k-1} \\ V_{a.k} = V_{rms.a} - n_{v.e}\cdot Q_{to} - n_{v.a}\cdot Q_{cir.a.k-1} \end{cases} \tag{28}$$

In (28), there exists the voltage bias caused by P_{to} and Q_{to}. Therefore, the steady-state voltage in the droop control should be adjusted as $V_{m.d.k}$. The phase $\theta_{d.k}$, angular frequency $\omega_{d.k}$ and RMS value $V_{A.d.k}$ of $V_{m.d.k}$ can be expressed as (29).

$$\begin{cases} \theta_{d.k} = \theta_{d.k-1} - m_{\omega.e}\cdot T_{c.\omega}\cdot P_{to} \\ \omega_{d.k} = \omega_d = \omega^* - m_{\omega.e}\cdot P_{to} \\ V_{A.d.k} = V_{A.d} = V_A - n_{v.e}\cdot Q_{to} \end{cases} \tag{29}$$

According to (29), the steady-state voltage error is determined by droop coefficients and output power. $\omega_{d.k}$ and $V_{A.d.k}$ are stable in the steady state (which are defined as ω_d and $V_{A.d}$), and $\theta_{d.k}$ varies with time ($t=k\cdot T_{c.\omega}$) because of the frequency bias.

Meanwhile, $V_{m.d.0}$ equals to V_m since the droop control don't work at the 0th control cycle, so $\theta_{d.0}$, $\omega_{d.0}$ and $V_{A.d.0}$ equal to 0, ω^* and V_A, according to the definition in Section II.

Moreover, the expression of $P_{cir.a}$ and $Q_{cir.a}$ shown in (22) should be adjusted because of the steady-state voltage bias. Meanwhile, the wire impedance is inductance (R_e=0) in the traditional droop control. Therefore, $P_{cir.a.k}$ and $Q_{cir.a.k}$ in the droop control can be simplified to (30).

$$\begin{cases} P_{cir.a.k} = \dfrac{k_a V_{A.d}^2}{\omega_d L_e}\cdot\left(\theta_{a.k}-\theta_{d.k}\right) \\ Q_{cir.a.k} = \dfrac{k_a V_{A.d}}{\omega_d L_e}\cdot\left(V_{a.k}-V_{A.d}\right) \end{cases} \tag{30}$$

Therefore, the general term formulas of $\theta_{a.k}$ and $V_{a.k}$ can be obtained as shown in (31) after substituting (30) into (28). This equation is the mathematical model of traditional droop control.

$$\begin{cases} \theta_{a.k} = \theta_{d.k} + \left(1 - \dfrac{m_{\omega.e}T_{c.\omega}V_{A.d}^2}{\omega_d L_e}\right)^k\cdot\theta_a \\ V_{a.k} = V_{A.d} + \left[1+\left(-\dfrac{n_{v.e}V_{A.d}}{\omega_d L_e}\right)^k\right]\cdot\dfrac{\omega_d L_e\left(V_{rms.a}-V_A\right)}{n_{v.e}V_{A.d}+\omega_d L_e} \end{cases} \tag{31}$$

According to this model, $\theta_{a.k}$ and $V_{a.k}$ should be convergent sequences in order to keep VSIPS stable. $m_{\omega.e}$ and $n_{v.e}$ should satisfy the relation of (32), and the convergent limits of $\theta_{a.k}$ and $V_{a.k}$ can be expressed as (33).

$$\begin{cases} 0 < m_{\omega.e} < \dfrac{2\omega_d L_e}{T_{c.\omega}V_{A.d}^2} \\ -\dfrac{\omega_d L_e}{V_{A.d}} < n_{v.e} < \dfrac{\omega_d L_e}{V_{A.d}} \end{cases} \tag{32}$$

$$\begin{cases} \lim\limits_{k\to\infty}\theta_{a.k} = \theta_{d.k} \\ \lim\limits_{k\to\infty}V_{a.k} = V_{A.d} + \dfrac{\omega_d L_e\left(V_{rms.a}-V_A\right)}{n_{v.e}V_{A.d}+\omega_d L_e} \end{cases} \tag{33}$$

As shown in (33), the convergent limit of $V_{a.k}$ doesn't equal to $V_{A.d}$. And the convergence limit of $Q_{cir.a}$ can be expressed as (34). According to (34), $Q_{cir.a}$ can be reduced by increasing $n_{v.e}$ or L_e, but can't be eliminated.

$$\lim_{k\to\infty} Q_{cir.a.k} = \lim_{k\to\infty} \frac{k_a V_{A.d}\left(V_{a.k} - V_{A.d}\right)}{\omega_d L_e} = \frac{k_a V_{A.d}\left(V_{rms.a} - V_A\right)}{n_{v.e} V_{A.d} + \omega_d L_e} \quad (34)$$

Based on the mathematical model of traditional droop control, the tradeoff between steady-state voltage error and load sharing accuracy is elaborated, and it is proved that V–Q droop control can't realize accurate reactive-power sharing.

V. Proposed Accurate Power-sharing Control Method

The proposed control method is expressed as (35), which is named as ω–P_{cir} and V–Q_{cir} control. In phasor model, ω–P_{cir} control can be transformed to (36). According to (35) and (36), there is no voltage bias and the steady-state voltage of VSIPS in the proposed method equals to V_m.

$$\begin{cases} \omega_{a.k} = \omega^* - m_{\omega.a} \cdot P_{cir.a.k-1} \\ V_{a.k} = V_{a.k-1} - n_{v.a} \cdot Q_{cir.a.k-1} \end{cases} \quad (35)$$

$$\theta_{a.k} = \theta_{a.k-1} - m_{\omega.a} \cdot T_{c.\omega} \cdot P_{cir.a.k-1} \quad (36)$$

The expression of $P_{cir.a}$ and $Q_{cir.a}$ can be simplified to (37). After substituting (37) into (35) and (36), the general term formulas of $\theta_{a.k}$ and $V_{a.k}$ can be expressed as (38), which is the mathematical model of proposed method.

$$\begin{cases} P_{cir.a.k} = \dfrac{k_a V_A^2}{\omega L_e} \cdot \theta_{a.k} \\ Q_{cir.a.k} = \dfrac{k_a V_A}{\omega L_e} \cdot \left(V_{a.k} - V_A\right) \end{cases} \quad (37)$$

$$\begin{cases} \theta_{a.k} = \left(1 - \dfrac{m_{\omega.e} T_{c.\omega} V_A^2}{\omega L_e}\right)^k \cdot \theta_a \\ V_{a.k} = V_A + \left(1 - \dfrac{n_{v.e} V_A}{\omega L_e}\right)^k \cdot \left(V_{rms.a} - V_A\right) \end{cases} \quad (38)$$

According to this model, $\theta_{a.k}$ and $V_{a.k}$ should be convergent sequences in order to keep VSIPS stable. $m_{\omega.e}$ and $n_{v.e}$ should satisfy the relation of (39), and the convergent limits of $\theta_{a.k}$ and $V_{a.k}$ can be expressed as (40). According to (40), these convergent limits equal to the phase and RMS value of V_m, so $P_{cir.a}$ and $Q_{cir.a}$ can be eliminated by proposed method.

$$\begin{cases} 0 < m_{\omega.e} < \dfrac{2\omega L_e}{T_{c.\omega} V_A^2} \\ 0 < n_{v.e} < \dfrac{2\omega L_e}{V_A} \end{cases} \quad (39)$$

$$\begin{cases} \lim\limits_{k\to\infty} \theta_{a.k} = 0 \\ \lim\limits_{k\to\infty} V_{a.k} = V_A \end{cases} \quad (40)$$

According to the characteristic of convergent sequence, the convergent rate is the fastest when $m_{\omega.e}$ and $n_{v.e}$ equal to m_T and n_T respectively, as shown in (41). Therefore, m_T and n_T are the optimum droop coefficient in the proposed method.

$$\begin{cases} m_T = \dfrac{\omega L_e}{T_{c.\omega} V_A^2} \\ n_T = \dfrac{\omega L_e}{V_A} \end{cases} \quad (41)$$

Therefore, the steady-state voltage error of droop control can be eliminated, and the accurate active and reactive power sharing can be realized.

VI. Simulation Results

A. Simulation of steady-state model and small-signal model

A simulation platform consisted of five ideal voltage-sources is established in PLECS in order to verify the proposed models. This platform's diagram is the same as Fig. 1, and simulation results are shown as follows.

In the steady-state model, the ideal voltage-sources equal to V_m, of which the RMS value is 110 V, frequency is 50Hz and phase angle is 0. The wire impedance and weighted coefficient k_a of inverters are listed in TABLE I.

TABLE I. Parameters of Simulation Parameter

	No.1	*No.2*	*No.3*	*No.4*	*No.5*
Wire inductance (μH)	100	200	300	400	500
Wire resistance ($m\Omega$)	0.1	0.2	0.3	0.4	0.5
Weight coefficient k_a	60/137	30/137	20/137	15/137	12/137

When Z_{load} is 3Ω, the waveforms of $I_{o.a}$ and $I_{cir.a}$ are shown in Fig. 6. According to simulation results, RMS value of I_{load} is 54.9963A, and RMS value of $I_{o.a}$ is 24.0860A, 12.0430A, 8.0287A, 6.0215A and 4.8172A respectively. These results showed that, $I_{o.a}$ satisfies the relationship of (3), which proved the proposed steady-state model.

Moreover, $I_{cir.a}$ is very small in the steady state according to Fig. 6, which proved the proposed small-signal model of circulating current.

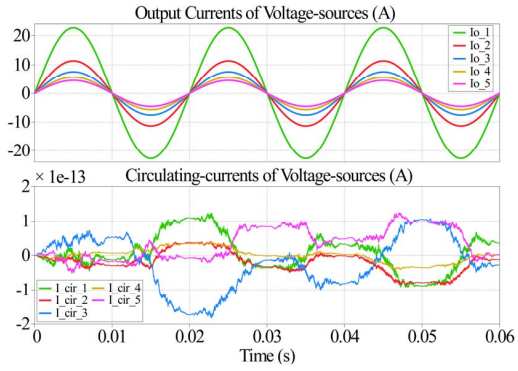

Fig. 6. Simulation results of steady-state model

B. Simulation of the circulating-current power model

In this simulation, the parameters of platform are listed in TABLE II. Therefore, V_m can be calculated by (11), of which the RMS value is $110V$ and the phase is 0. When Z_{load} is 3Ω, the waveforms of $I_{o.a}$ and $I_{cir.a}$ are shown in Fig. 7.

TABLE II. PARAMETERS OF SIMULATION PLATFORM

	No.1	*No.2*	*No.3*	*No.4*	*No.5*
RMS of voltage (V)	109.9	109.95	110	110.05	110.1
Phase of voltage (rad)	1×10^{-4}	2×10^{-4}	0	-2×10^{-4}	-1×10^{-4}
Wire inductance (μH)	200	100	50	100	200
Wire resistance ($m\Omega$)	0.2	0.1	0.05	0.1	0.2
Weight coefficient k_a	0.1	0.2	0.3	0.2	0.1

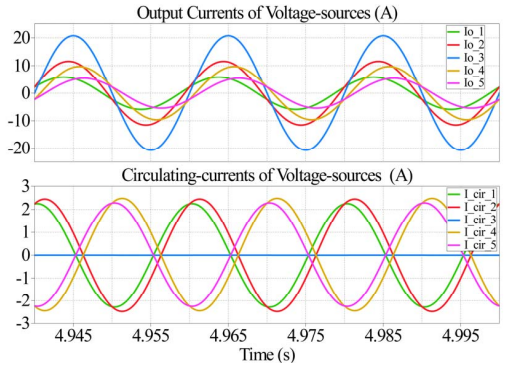

Fig. 7. Simulation results of small-signal mode

According to (22), the theoretical value of $P_{cir.a}$ and $Q_{cir.a}$ can be calculated as shown in TABLE III.

TABLE III. THEORETICAL VALUES OF $P_{cir.a}$ AND $Q_{cir.a}$

	No.1	*No.2*	*No.3*	*No.4*	*No.5*
$P_{cir.a}$ (W)	18.700	76.473	0.000	-76.473	-18.700
$Q_{cir.a}$ (Var)	-175.007	-174.823	0.000	174.823	175.007

Meanwhile, the simulation results of $P_{cir.a}$ and $Q_{cir.a}$ with different load are listed in TABLE IV and V respectively, which are calculated by (19).

TABLE IV. SIMULATION RESULTS OF $P_{cir.a}$ (W)

R_{load} (Ω)	*No.1*	*No.2*	*No.3*	*No.4*	*No.5*
1	17.584	75.329	0.041	-75.358	-17.597
3	18.318	76.065	0.041	-76.093	-18.331
12	18.593	76.34	0.041	-76.368	-18.606

TABLE V. SIMULATION RESULTS OF $Q_{cir.a}$ (Var)

R_{load} (Ω)	*No.1*	*No.2*	*No.3*	*No.4*	*No.5*
1	-174.8	-174.8	-0.198	174.77	175.07
3	-174.9	-175.1	-0.198	175.09	175.14
12	-175	-175.2	-0.198	175.21	175.17

According to these tables, simulating result of circulating-current power is close to the theoretical result, which can prove the accuracy of the circulating-current power model.

Meanwhile, simulation result of circulating-current power is influenced by Z_{load}. The smaller Z_{load} is, the larger the error of simulation result is. Therefore, the equivalent wire impedance of parallel system should be far less than Z_{load} in order to reduce the influence of load.

C. Simulation of the proposed method

A simulation platform consisting of two inverters is established in PLECS. The inverter parameters are listed in TABLE VI. Z_{load} is 4.1Ω. The RMS values of two inverters are set as $109.8V$ and $110.2V$ respectively, and the phase difference is set as $0.0314rad$.

TABLE VI. PARAMETERS OF TWO INVERTERS

	Parameters	*Value*	*Unit*
1	weight coefficient (k_a)	0.5	
2	RMS of steady-state voltage (V_A)	110	V
3	Output frequency (f_o)	50	Hz
4	Droop cofficient of $\omega-P$ or $\omega-P_{cir}$ ($m_{\omega.a}$)	1×10^{-4}	$2\pi\times Hz/W$
5	Droop cofficient of $V-Q$ or $V-Q_{cir}$ ($n_{v.a}$)	1×10^{-3}	V/Var
6	Wire inductance ($L_{w.a}$)	250	μH
7	Wire resistance ($R_{w.a}$)	0	Ω

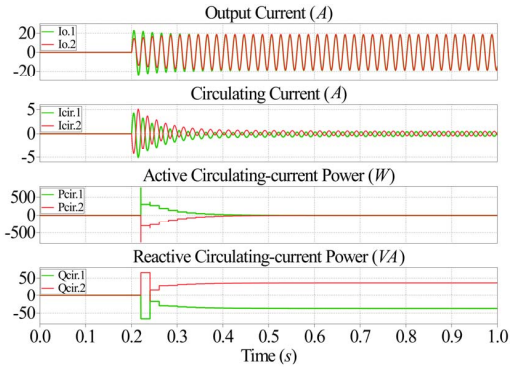

Fig. 8. Simulation result of the droop control

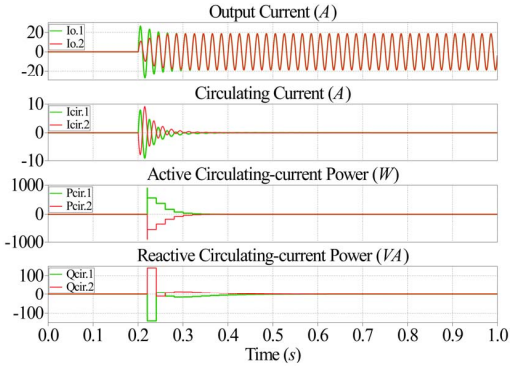

Fig. 9. Simulation result of the proposed method

Fig. 8 and Fig. 9 show the simulation results of the droop control and the proposed method respectively. Comparing these figures, there are obvious circulating currents in Fig. 8, which are reduced substantially in Fig. 9.

Moreover, Q_{cir} of two inverters in the steady-state are about $37Var$ and $-37Var$ in droop control, which is calculated by PLECS. While in the proposed method, both P_{cir} and Q_{cir} equal to 0 approximately.

VII. Experiment Results

An experiment platform consisting of two parallel-inverter prototypes is established. The inverter parameters are the same as TABLE VI, and Z_{load} is 5.1Ω.

Fig. 10 shows the experiment result in the droop control, and Fig. 11 shows that in the proposed method. Comparing these figures, there are obvious circulating currents in the droop control, which are reduced substantially in the proposed method.

Meanwhile, the measured values of $Q_{cir.1}$ and $Q_{cir.2}$ in the steady-state are $93Var$ and $-93Var$ in droop control. While in proposed method, both P_{cir} and Q_{cir} equal to 0 approximately.

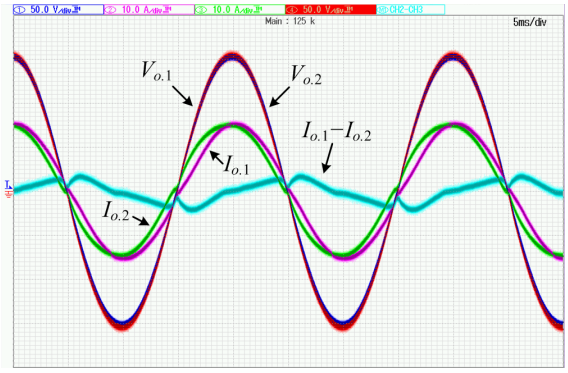

Fig. 10. Experiment result of droop control

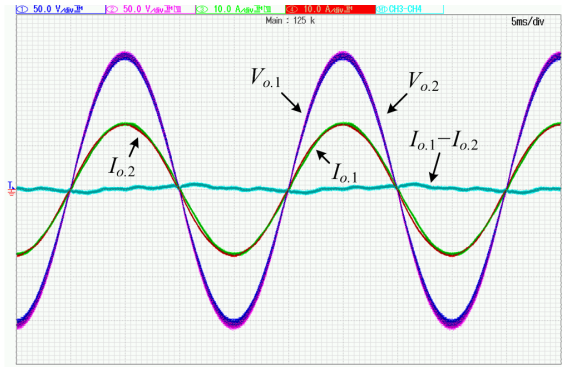

Fig. 11. Experiment result of proposed method

VIII. Conclusions

This paper analyzed the parallel system as a multi-input & multi-output system, and proposed a mathematical model of circulating current, the steady-state model and small-signal model of parallel system. Then the phasor models of circulating-current and circulating-current power are proposed.

Subsequently, the model of traditional droop cpntrol is built and analyzed based on the circulating-current power model. According to this model, the tradeoff between steady-state voltage error and load sharing accuracy is elaborated, and it is proved that $V-Q$ droop control can't realize accurate reactive-power sharing.

According to the analysis of droop control, an accurate power-sharing control method ($\omega-P_{cir}$ and $V-Q_{cir}$ control) is proposed in this paper. Subsequently, the mathematical model of the proposed method is built and analyzed based on circulating-current power model, which proves that it can eliminate the circulating-current power and the bias of output voltage frequency and amplitude. Finally simulation and experiment results are presented, which validate the performance of the proposed method.

Acknowledgment

The authors would like to thank Technology Dynamics Inc., for the support of the inverter power stage during the project. The authors also would like to thank PLEXIM Inc., for the support of the powerful simulation tools PLECS.

References

[1] Peng, F.Z., Yun Wei Li, Tolbert, L.M., "Control and protection of power electronics interfaced distributed generation systems in a customer-driven microgrid," Power & Energy Society General Meeting, 2009. PES '09. IEEE , vol., no., pp.1,8, 26-30 July 2009

[2] De Brabandere K.., Bolsens B.., Van den Keybus J.., Woyte A.., Driesen J.., Belmans R.., "A Voltage and Frequency Droop Control Method for Parallel Inverters", IEEE Transactions on Power Electronics, vol. 22, no. 4, pp. 1107–1115, July 2007.

[3] J. M. Guerrero, Luis García de Vicuña, José Matas, Miguel Castilla, and Jaume Miret," Output Impedance Design of Parallel-Connected UPS Inverters With Wireless Load-Sharing Control", IEEE Transactions on Industrial Electronics, vol. 52, no. 4, pp. 1126–1136, Aug. 2005.

[4] Guerrero, J.M., Matas, J., De Vicuna, L.G., Berbel, N., Sosa, J., "Wireless-control strategy for parallel operation of distributed generation inverters," Industrial Electronics, 2005. ISIE 2005. Proceedings of the IEEE International Symposium on , vol.2, no., pp.845,850 vol. 2, 20-23 June 2005

[5] Lee, C-.T., Chu, C-.C., Cheng, P-.T., "A New Droop Control Method for the Autonomous Operation of Distributed Energy Resource Interface Converters," Power Electronics, IEEE Transactions on , vol.28, no.4, pp.1980,1993, April 2013

[6] Wei Yao, Min Chen, Matas, J., Guerrero, J.M., Zhao-ming Qian, "Design and Analysis of the Droop Control Method for Parallel Inverters Considering the Impact of the Complex Impedance on the Power Sharing," Industrial Electronics, IEEE Transactions on , vol.58, no.2, pp.576,588, Feb. 2011